Toroidal versus Spiral Inductors in Multilayered Tecnologies

José M. Lopez-Villegas [#1], Neus Vidal [#2], Jesús A. del Alamo [*3]
[#] RF Lab, Electronics Department, University of Barcelona, Spain
[*] Microsystem Technology Labs, Massachusetts Institute of Technology, Cambridge MA, USA
[1] jmlopez@el.ub.edu, [2] nvidal@ub.edu, [3] alamo@mit.edu

***Abstract*—This work is aimed to compare the performance of toroidal inductors and planar spiral inductors in multi-layered technologies. Toroidal inductors are investigated theoretically, and closed formula is derived for the inductance as a function of geometrical parameters. The obtained model is validated by experimental results and EM simulation. From the comparison of the inductance of toroidal inductors and compact spiral inductors, a selection rule is proposed to choose the most suitable topology that leads to the most compact design.**

***Index Terms*—Inductance calculation, Inductor design, Toroidal inductor, Inductor selecting rule.**

I. Introduction

Toroidal inductors and transformers in discrete form are widely used in low frequency power electronics applications. One prime example of such applications is power conversion. An increase in switching frequency allows greater compactness and also yields better performance in power converters [1], [2]. Increasing switching frequency means less demand for energy storage and consequently smaller values of the passive components. However, it is not clear how the size of passive components scales down with increasing frequency, without degrading their overall performance.

In the RF band of the electromagnetic spectrum, planar spiral inductors have been widely used in the design of radio frequency integrated circuits (RFICs) intended to work in the GHz range and beyond [3], [4]. The main concern when using these passive components is area consumption. Scaling-down frequency means the need of higher values of inductance that can only be achieved by increasing the number of turns of the coils. This leads to an increase in losses and area, which makes their use less attractive.

According to this, at intermediate frequencies that are likely to become relevant for future power switching applications based on novel GaN power transistors, it is not clear which of these inductor designs, toroidal or planar spiral, is preferable. These intermediate frequencies would roughly correspond to very high frequency (VHF) band from tens of MHz to few hundreds of MHz However, there are not yet clear criteria on what inductor topology to choose for a given application. Contributing to the establishment of such criteria is the main objective of this work.

In Section II a model for multilayered toroidal inductors is presented and validated by experimental data and simulation results. Section III presents the results of the comparison of toroidal and spiral inductors, in terms of achievable inductance. Inductor selection rule as a function of geometrical parameters is also presented and discussed in this section. Finally, Section IV concludes the paper.

II. Multilayer Toroidal Inductor Modelling

Fig. 1 shows an example of a toroidal inductor constructed using strips on the top and bottom surfaces of a multilayer substrate. Via holes through the substrate are used to close each turn. On the left side a via hole is removed to provide a feed point for current injection. Provided the number of turns is high enough (i.e. N>>1) the inductance of this toroid is given by [5], [6]:

$$L = \mu \frac{N^2 h}{2\pi} \ln\left(\frac{b}{a}\right) + L_o \qquad (1)$$

Where, μ is the substrate permeability, N is the number of turns, h is the substrate thickness, a and b are the inner and outer radii, respectively, and L_o, is the inductance of the spur-shaped loop that remains when the substrate

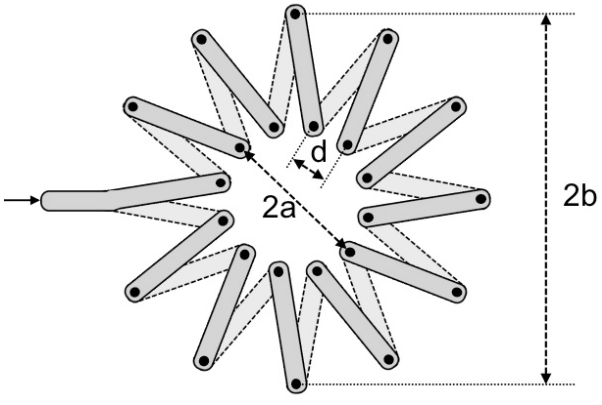

Fig. 1. Schematic view of a toroidal Inductor in multilayer technology

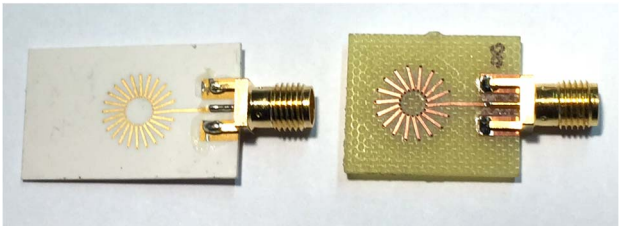

Fig. 2. Implementation of toroidal Inductors in multilayer technologies. On the left using LTCC technology. On the right using standard PCB technology.

thickness *h* collapses to zero.

Expression (1) can be rewritten in a more convenient way if we perform an in-depth analysis of the toroid geometry shown in Fig. 1. The most important parameter is the minimum distance between via holes, *d*. For instance, given a number of turns, *N*, and the inner radius *a* of the toroid it holds that:

$$2\pi a \approx Nd \tag{2}$$

By replacing (2) in (1) and using the ratio $R=a/b$, we finally obtain the following expression for the inductance:

$$L = \mu \frac{\pi b^2 h}{d^2} R^2 \ln\left(\frac{1}{R^2}\right) + L_o \tag{3}$$

Fig. 2. shows two examples of toroidal inductors. The first one on the left has been implemented using Low Temperature Co-fired Ceramics (LTCC) technology and the second on the right using Printed Circuit Board (PCB) technology. Fig. 3 shows the equivalent inductance and the quality factor of the LTCC inductor of Fig. 2 Thin red line corresponds to raw data before de-embedding the SMA connector and pad effects from the S parameter measurements. Thick black line corresponds to data after de-embedding. In Fig. 4 the DC limit of the equivalent inductance of a set of PCB toroidal inductors is plotted as a function of the number of turns. In all cases, the external radius is b=4.7 mm, the minimum distance between via holes is d=0.6 mm, and the metal strip width is w=0.45 mm. Data obtained from experimental measurements are plotted using solid symbols. Outlined symbols are used for data obtained from Momentum electromagnetic simulations. Three substrate thicknesses with the are considered: h=1.57 mm, h=0.83 mm and h≈0. The last case emulates the substrate collapsing to zero thickness with the top and bottom metal strips of the toroids having merged together on the top surface. Accordingly, the obtained values of the inductance when h≈0 correspond to, L_o. Finally, Fig. 5 shows the corrected values of the DC limit of the equivalent inductance by subtracting L_o. Experimental data and simulation results are compared

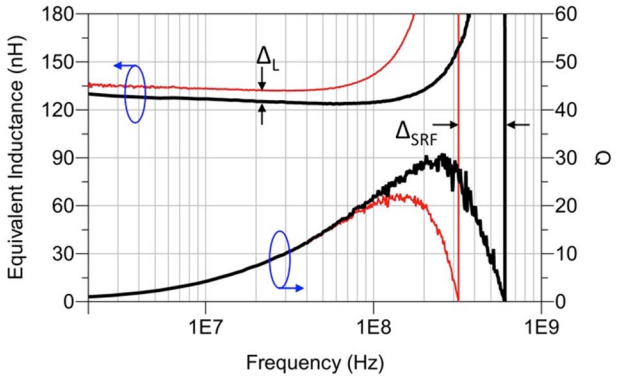

Fig. 3. Equivalent Inductance and Quality Factor as a function of frequency for a LTCC toroidal inductor, thin red line corresponds to raw data before de-embedding of SMA connector and pad effects from the measured S parameters. Thick black line corresponds to data after de-embedding.

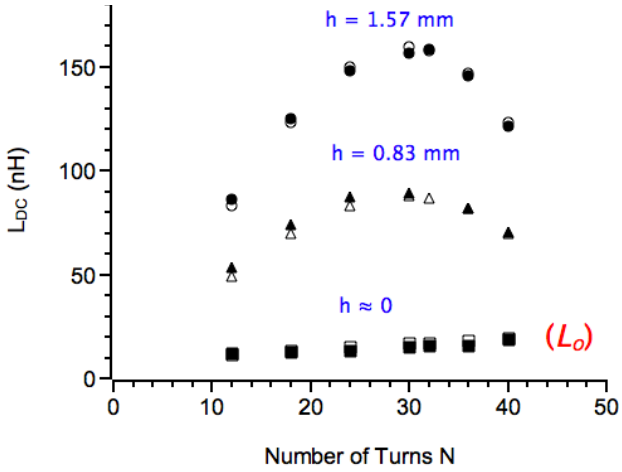

Fig. 4. Plot of the DC limit of the equivalent inductance of PCB single toroidal inductors as a function of the number of turns. Solid symbols correspond to experimental measurements. Outlined symbols correspond to simulation results.

with the prediction of the model derived from (3). It is important to remark the good agreement between data and theory, particularly since there are no fitting parameters.

We can observe a maximum of the corrected equivalent inductance of the toroidal inductor that according to (3) is equal to:

$$L_{max} = \mu \frac{\pi b^2 h}{d^2 e} \tag{4}$$

where, *e*, is Euler's number. The inductance maximum is achieved for an optimum value of the ratio, *R*, given by:

$$R_{opt} = \frac{1}{\sqrt{e}} = 0.6065\ldots \tag{5}$$

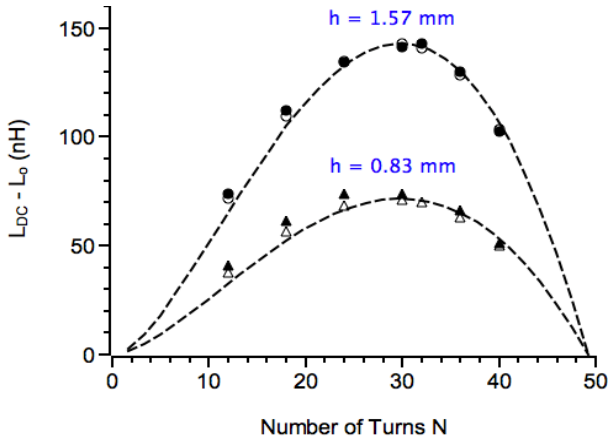

Fig. 5. Corrected values of the DC equivalent inductance of PCB toroids after removal of the spur-shape loop inductance, L_o. Solid symbols correspond to experimental measurements. Outlined symbols correspond to simulation results. Circles and triangles are the results for substrate thicknesses, h=1.57 mm, and, h=0.83 mm, respectively. Dashed lines are the theoretical curves derived from (3).

According to (5), for a given size (i.e. volume) of the toroidal inductor, the equivalent inductance achieves its maximum value when the inner radius, a, is about 60-61% of the external radius, b, regardless of the number of turns or metal strip width.

III. Toroidal vs. Spiral Inductors

To point out the advantages of using multilayer toroidal inductors it is mandatory to compare their performance with that of planar spiral inductors. Planar spiral inductors of different shapes (i.e. circular, octagonal, or square) have been used for decades in integrated and/or multilayer technologies [3], [4]. There is a vast literature available concerning the modelling of planar spiral inductors, including measurement fitting modelling, numerical simulations, and closed analytical formulae [7]. For our comparison with toroidal inductors we are going to use a proposed closed formula for planar spiral inductors that has been shown be rather accurate [8]. According to this work the inductance of compact planar spirals of circular shape can be written as:

$$L_{spiral} = k\,\mu\,\frac{b^3}{d^2} \qquad (6)$$

where k=0.55.

For comparison purposes, to derive (6) from the original formula in [7] we have assumed that the inner radius of the spiral is zero (i.e. compact inductor). Moreover, the strip with of the coil is that of the toroidal inductor and the pitch between turns is equal to the minimum distance between via holes, d, in the toroidal design.

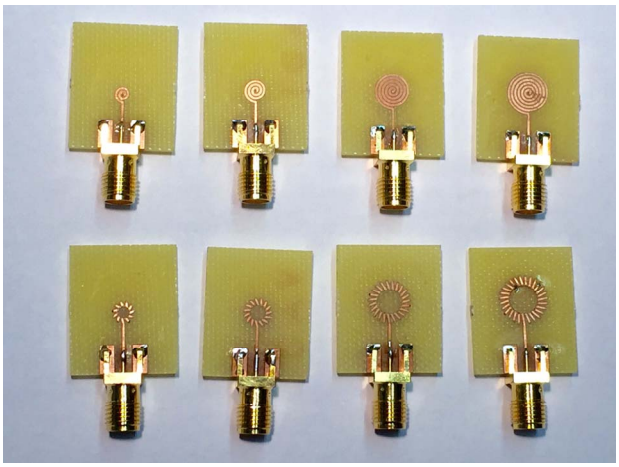

Fig. 6. PCB inductors used for the comparison of spiral and toroid geometries. In the first row they are compact spiral inductors of different sizes. In the second row some optimum toroidal inductors are shown.

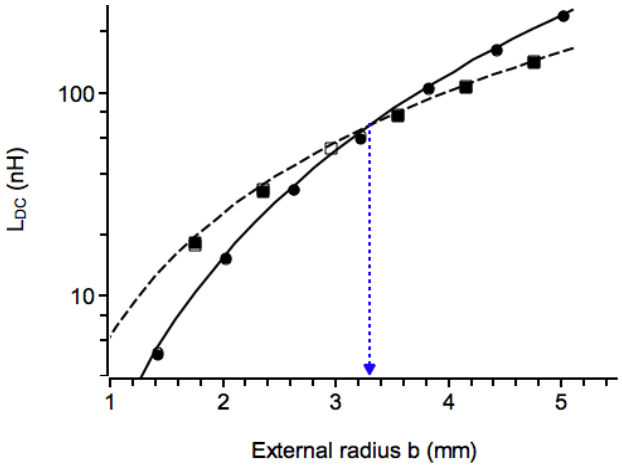

Fig. 7. DC equivalent inductance of PCB inductors as a function of the external radius, b. Solid symbols correspond to experimental measurements. Outlined symbols correspond to simulation results. Circles are spiral inductor results. Squares correspond to optimum toroidal results corrected from, L_o. Dashed curve is the theoretical dependence derived from (4). Continuous curve corresponds to the closed formula for compact circular spiral inductors in (6).

A set of compact spiral inductors of different sizes has been designed and fabricated using PCB technology. This set has been compared with other set of toroidal inductors having similar sizes and the optimum ratio, R_{opt}, so that the DC equivalent inductance reaches its maximum. Fig. 6. shows some of the fabricated devices.

In Fig. 7 the DC equivalent inductance is plotted against the external radius b for circular spiral and optimum toroidal inductors. A good agreement is observed between

experiments, simulations and theory. As expected, we can clearly see a different behavior for both inductor topologies. Spiral inductors show a stronger dependence on *b* than toroidal inductors. We can observe a cross point for an external radius b≈3.3 mm. Below this value the equivalent inductance of a toroidal inductor is bigger than that of a compact spiral of the same size, and viceversa.

In the general case, by dividing (6) over (4) we can obtain the ratio between the inductances of circular spiral inductor and optimum toroidal inductor corrected from, L_o, which is given by:

$$\frac{L_{spiral}}{L_{max}} = \frac{ke}{\pi}\,\frac{b}{h} \tag{7}$$

According to (7) the inductance ratio is proportional to the geometrical aspect ratio, *b/h*. The proportionality constant is ke/π=0.476. Fig. 8 shows the experimental inductance ratio as a function of the aspect ratio *b/h*. To obtain the inductance ratios at the same value of *b/h*, data corresponding to the spiral inductors have been fitted with a third order polynomial and then interpolated. In the same figure, the lineal theoretical dependence derived from (7) is also shown. A very good agreement is observed between measurements, and theory. We can observe that there is a threshold value of the ratio *b/h* equal to about 2.1 (i.e. the inverse of the proportionality constant in (7)) that defines a selection rule. Below this value the inductor topology of choice to achieve the highest inductance density is the toroid. Conversely, above the threshold spirals outperform toroidal counterparts.

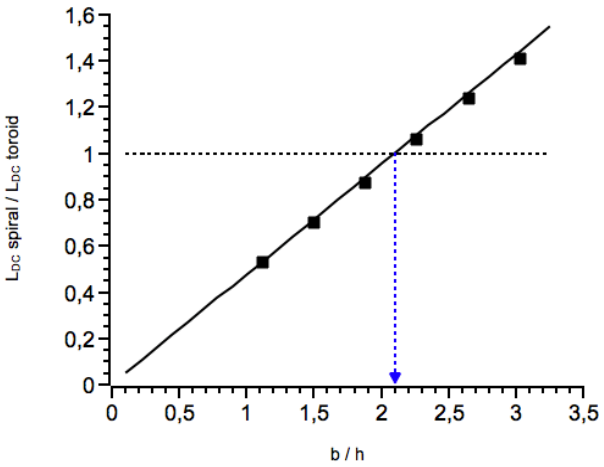

Fig. 8. DC equivalent inductance ratio of PCB inductors as a function of the inductor aspect ratio, *b/h*. Squares correspond experimental data. Continuous line corresponds to the lineal behavior derived from (7).

IV. Conclusion

In this work a model of embedded toroidal inductors in multilayered technologies is proposed and validated by experimental data and simulation results. Moreover, it has been demonstrated that the geometry of the toroid can be optimized to improve the maximum achievable inductance. The comparison in terms of achievable inductance of planar spiral inductors and toroidal inductors reveals that the key parameter is the aspect ratio, *b/h*. An inductor selection rule has been derived and experimentally validated to obtain the optimum designs that maximizes the inductance density. As far as we know this is the first proposed procedure to decide whether to use planar spiral or toroidal inductor geometry, for a given requirement of inductance value and fabrication technology.

Acknowledgment

This work was supported in part by the Spanish Secretary of State for Research, Development and Innovation Under Project TEC2013-40430-R, and by the Spanish Secretary of State for Education, Professional Training and Universities Under Project PRX12/00169.

References

[1] D. J. Perreault, J. Hu, J.M. Rivas, Y. Han, O. Leitermann, R.C.N. Pilawa-Podgurski, A. Sagneri, and C.R. Sullivan, "Opportunities and challenges in very high frequency power conversion," in *Proc. IEEE Appl. Power Electron. Conf. Expo., Feb. 2009, pp 1-14.*

[2] M. Araghchini, J. Chen, V. Doan-Nguyen, D.V. Harburg, D. Jin, J. Kim, M.S. Kim, S. Lim, B. Lu, D. Piedra, J. Qiu, J. Ranson, M. Sun, X. Yu, H. Yun, M.G. Allen, J.A. del Alamo, G. DesGroseilliers, F. Herrault, J.H. Lang, C. G. Levey, C.B. Murray, D. Otten, T. Palacios, D.J. Prreault, and C.R. Sullivan, "A technology overview of the powerchip development program," *IEEE Trans. Power Electronics*, vol. 28, no. 9, pp. 4182–4201, Sept. 2013.

[3] J.N. Burghartz, and B. Rejaei, "On the design of RF spiral inductors on silicon," *IEEE Trans. Electron Devices*, vol. 50, no. 3, pp. 718–729, Mar. 2003.

[4] J.N. Burghartz, D.C. Edelstein, M. Soyuer, H.A. Ainspan, and K.A. Jenkins, "RF circuit design aspects of spiral inductors on silicon," *IEEE J. Solid-State Circuits*, vol. 33, no. 12, pp. 2028–2034, Dec. 1998.

[5] E.B. Rosa, "The self-inductance of a toroidal coil of rectangular section", *Bulletin of the Bureau of Standards*, vol. 4, no 1, pp. 141-148, 1907.

[6] J. Pejtersen, and, A. Knott, "Design and measurement of planar toroidal transformers for very high frequency power applications," in *Proc. IEEE 7th Inter. Power Electron. And Motion Control Conf., 2012, pp 688-692.*

[7] J.J. Sieiro, J.M. Lopez-Villegas, J. Cabanillas, J.A. Osorio and J. Samitier, "A Physical Frequency-Dependent Compact Model for RF Integrated Inductors," *IEEE Trans. Microwave Theory Tech.,* vol. 50, pp 384-392, Jan. 2002.

[8] S. S. Mohan, M. M. Hershenson, S. P. Boyd, and T. H. Lee, "Simple accurate expressions for planar spiral inductors," *IEEE J. Solid-State Circuits*, vol. 34, pp. 1419–1425, Oct. 1999.